Bioorganic & Medicinal Chemistry 19 (2011) 7501–7506

Contents lists available at SciVerse ScienceDirect

Bioorganic & Medicinal Chemistry

journal homepage: www.elsevier.com/locate/bmc

Structure-based rational design of novel hit compounds for pyruvate dehydrogenase multienzyme complex E1 components from *Escherichia coli*

Yanliang Ren [†], Junbo He [†], Lingling Feng, Xun Liao, Jing Jin, Yongjian Li, Yi Cao, Jian Wan [*], Hongwu He [*]

Key Laboratory of Pesticide and Chemical Biology (CCNU), Ministry of Education, Department of Chemistry, Central China Normal University, Wuhan 430079, China

ARTICLE INFO

Article history:
Received 15 September 2011
Revised 11 October 2011
Accepted 13 October 2011
Available online 19 October 2011

Keywords:
Pyruvate dehydrogenase
Structure-based molecular docking
Molecular dynamics simulation
Fragment molecular orbital

ABSTRACT

Pyruvate dehydrogenase multienzyme complex (PDHc) E1 component plays a pivotal role in cellular metabolism to convert the product of glycolysis (pyruvate) to acetyl-CoA, and has been reported as a potential target for anti-microbial and herbicide. In present study, based on the thiamin diphosphate (ThDP) site, four novel hit compounds with high inhibitory activity against the PDHc-E1 from *Escherichia coli* were firstly designed by using structure-based molecular docking methods. As expected, among four compounds, the compound **3a** is the best inhibitor by far, with IC_{50} value of 6.88 μM against PDHc-E1 from *E. coli*. To elucidate the interaction mechanism between the active site of PDHc-E1 and its inhibitor, the docking-based molecular dynamics simulation (MD) and MD-based ab initio fragment molecular orbital (FMO) calculations were also further performed. The positive results indicated that all modeling strategies presented in the current study most like to be an encouraging way in design of novel lead compounds with structural diversity for PDHc-E1 in the future.

1. Introduction

Pyruvate dehydrogenase multienzyme complex (PDHc) plays a pivotal role in the oxidation of pyruvate acid to acetyl-CoA, one of the two compounds needed for condensation to citrate and required for tricarboxylic acid metabolic cycle. The fundamental reactions of this complex are carried out by three enzymatic components: pyruvate dehydrogenase (E1), dihydrolipoamide acetyltransferase (E2), and dihydrolipoamide dehydrogenase (E3).[1] The E1 component catalyzes the first step of the multistep process. PDHc-E1 enzyme has been reported[2] as the potent anti-microbial and herbicide targets for a long time. Both thiamin diphosphate (ThDP) and Mg^{2+} are essential cofactors be involved in the hysteretic regulation of PDHc-E1 activity.[3] As would be expected, blocking the active site of cofactor, for example, by replacing it with inhibitors, inactivates the enzyme.

Great efforts have been made to design, synthesize and develop the inhibitor of PDHc-E1, such as substrate analogs including bromopyruvate,[4] fluoropyruvate,[5,6] the phosphonate,[7] and phosphinate analogs of pyruvate,[8] mono- and bifunctional arsenoxides,[9,10] branched-chain 2-oxo acids,[11] 2-oxo-3-alkynoic acids.[12] Recently, the investigations of PDHc-E1 cofactor (ThDP) analogs have been received more and more attentions, because of their high binding affinities against PDHc-E1 enzyme, such as tetrahydrothiamin diphosphate,[13–15] 2-thiazolone and 2-thiothiazolone analogs of ThDP.[16] There is, however, no commercial potent inhibitors situated in the ThDP binding site of PDHc-E1. It is interesting to design and synthesis PDHc-E1 inhibitors based on the structure of coenzyme and properties of the active site.

To design high-effective inhibitors, the knowledge of binding interaction between inhibitors and active site of target enzyme is essential. So far, the X-ray crystal structure of PDHc-E1/ThDP complex from *Escherichia coli* (PDB ID: 1L8A[17]) were determined, which not only increased the better understandings into PDHc-E1 structure and its catalysis mechanism, but also help to develop novel broad-spectrum inhibitors[17] with high inhibitory activities on PDHc-E1 and better pharmaceutical properties.

The main purpose of this study was to elucidate the interaction mechanism between ligands and active site of PDHc-E1 to give better information for designing the reasonable inhibitors in future. In present study, by jointly using the molecular docking, molecular dynamics (MD), fragments molecular orbital (FMO) method, four hit compounds were designed for the first, subsequently were synthesized. The PDHc-E1 inhibitory assay in vitro for these compounds have been tested, the higher inhibitory activity of these compounds against PDHc-E1 from *E. coli* lending credit to our current attempts in quest for potential PDHc-E1 inhibitors with new active pharmacophore.

* Corresponding authors. Tel./fax: +86 27 67862022.
E-mail addresses: jianwan@mail.ccnu.edu.cn (J. Wan), he1208@mail.ccnu.edu.cn (H.W. He).
† These authors contributed equally to this study.

0968-0896/$ - see front matter © 2011 Elsevier Ltd. All rights reserved.
doi:10.1016/j.bmc.2011.10.035

2. Results and discussion

2.1. Chemistry

The synthetic route employed to obtain the title compounds **3a**–**e** is depicted in Scheme 1. Four alkyne precursors **1a**–**d** were synthesized from the 3-bromopropyne with corresponding substituted phenol in refluxing acetone with K_2CO_3 as base. The 5-azidomethyl-2-methylpyrimidine-4-ylamine **2** was prepared readily from thiamine hydrochloride according to the literature method as described.[18] The Cu-catalyzed 1,3-dipolar cycloaddition[19] was introduced to assemble the final target compounds **3a**–**d**. A combination of copper(II) sulfate/sodium ascorbate was utilized in situ to prepare the copper(I) species, and a 'click chemistry' was achieved in 12 h at room temperature. Compound **3d** was hydrolyzed by LiOH to give compound **3e**.

2.2. Structure-based docking

To validate the reliability of the structure-based docking methodology adopted herein, the cofactor ThDP in the X-ray crystallographic structure of 1L8A was taken as a testing molecule. The initial geometric parameters of ThDP backbone was extracted from 1L8A, the hydrogen atoms were added and minimized by using the SYBYL7.3 package, and then ThDP was docked backing into the active site of 1L8A by the SURFLEX module. The structure parameters of enzyme were set rigid, while the ThDP parameters were set flexible during the present molecular docking process. The molecular docking results revealed that the binding mode of ThDP obtained by SURFLEX was almost identical to those of crystal complex with rmsd 3.2 Å (as illustrated in Fig. 1), which implied that the binding mode of ThDP docked by the SURFLEX module was most likely valid. Therefore, by using same docking procedure, the four novel hit compounds were designed and docked in the present study. As shown in Figure 2, our designing compound **3a** with highest inhibitory activity (IC_{50} = 6.88 μM) is occupy the ThDP-binding pocket of PDHc-E1, thereby blocking the ThDP access to PDHc-E1. Similar to the binding mode of crystal ThDP in active site of PDHc-E1, the compound **3a** are also bound in a pocket of PDHc-E1 with the 'V' conformation. On the right side of 'V' conformation, the strong π–π stacking between the aminopyrimidine ring of the compound **3a** and the side chain ring of Phe602 is evident. Also, several hydrogen bonds participate in binding the aminopyrimidine ring. The amino group connected to the pyrimidine ring forms a hydrogen bond with the main chain oxygen of Val192. Another two key hydrogen bonding interaction (conserved in all ThDP dependent enzymes of known structure) is made by N1′ of the pyrimidine ring with the side chain of Glu571 and N2′ of the pyrimidine ring with the Met194. Our docking results analyses suggest that the hydrogen bonds and π–π stacking mentioned above are responsible for the proper orientation of aminopyrimidine of the inhibitor in the active site, as shown in dashed lines in Figure 2.

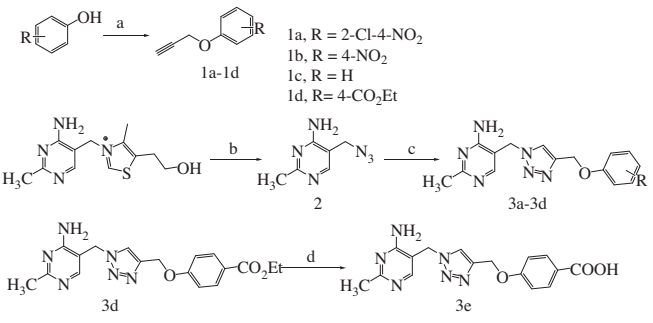

Scheme 1. Reactions and conditions (a) 3-bromopropyne, K_2CO_3, acetone, reflux, 5 h; (b) NaN_3, Na_2SO_3, H_2O, 60–65 °C, 6 h, 63%; (c) **1a**–**d**, sodium ascorbate, $CuSO_4{\cdot}5H_2O$, *t*-BuOH/H_2O (2:1), rt, 12 h; (d) LiOH, THF/MeOH/H_2O (2:1:1), rt, 12 h.

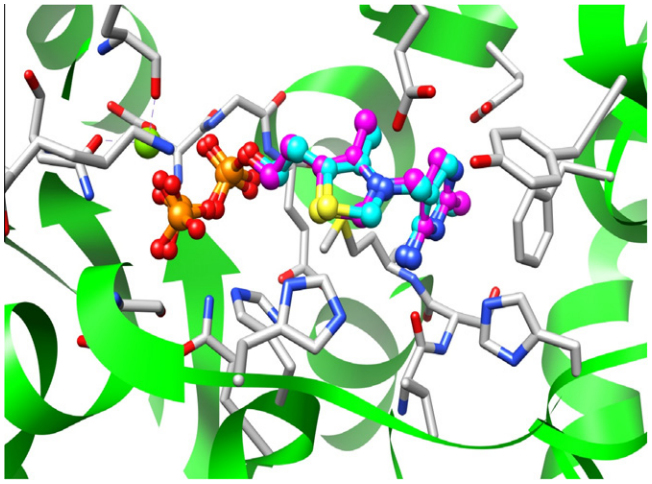

Figure 1. Schematic for the validation of molecular docking procedures of SURFLEX module, in which docking conformation (pink) versus crystal binding conformation (light blue) for the cofactor ThDP in the active site of PDHc-E1 from *E. coli*.

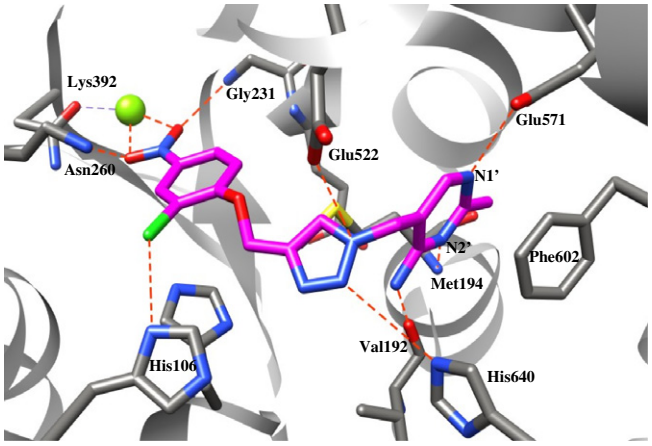

Figure 2. Optimal binding model for compound **3a** into active site of PDHc-E1 from *E. coli* docked by SURFLEX module, in which PDHc-E1 is shown in ribbon, ligand and some key residues are shown in stick, both coordination bonds and hydrogen bonds are shown in dashed lines (red).

On the middle of the 'V' conformation, the triazole in the compound **3a** forms two hydrogen bond with the residues Glu522 and His640, respectively. It should be noted that the residue His640 can also form hydrogen bond with the pyruvate acid and partly responsible for its proper orientation,[17] to some extend, the compound **3a** likely occupy part of the binding site for substrate pyruvate acid.

On the left side of compound **3a**, our docking results show that the nitryl group on benzene ring not only form three hydrogen bonds with Gly231, Asn260 and Lys392, but also coordinate with the Mg^{2+} in the active site. The chlorine atom connected to benzene also likely form one hydrogen bond with the nearby residue His106. Furthermore, the benzene group appears form π–π stacking with residue His106.

2.3. Molecular dynamics (MD) simulation

In the docking studies, flexibility of the protein was not taken into account. To insight into the reasonable binding models of

inhibitors in active site, the docking complex 1L8A/compound **3a** was subjected to 1400 ps MD simulations, the RMSDs of the entire enzyme backbone (contain the ligand) with respect to the stating structure of receptor was calculated by using the PTRAJ module of AMBER 8.0. As illustrated in Figure 3A, the whole system arrived at a dynamic convergence with the rmsd around 1.9–2.0 Å.

An average conformation of PDHc-E1 was derived from 885 to 985 ps in simulation trajectory and subjected to a subsequent minimization using Tripos force field of SYBYL7.3 with a rms gradient of 0.05 kcal/(mol Å), as shown in Figure 3B. The direct interactions between compound **3a** and the key residues in active site of PDHc-E1 for docking conformation and docking-based MD conformation are list in Table 2. We can find in Table 2 that, on the right side of 'V' conformation of compound **3a**, the bond distances from aminopyrimidine to residues Glu571, Met194, Val192 and Phe602 exhibited subtle changes (0.05–0.5 Å) when the MD simulation was performed, thus it again cleared that these four residues are well conserved and might function in stabilization of aminopyrimidine. On the left side of 'V' conformation, there are two important bond distance exhibit subtle changes, one is the coordinate bond between the nitryl group and Mg^{2+}, with a change of −0.05 Å; another is the hydrogen bond between nitryl group and residue Asn260, with a change of 0.5 Å. The consistence between docking results and MD simulation results revealed that these hydrogen-bond and coordinate-bond are much important for stabilizing the compound **3a**. Furthermore, it is notable that MD simulation result in a new and stable hydrogen-bond between nitryl group of the compound **3a** and the residue Gln140 was formed, with a bond distance of 2.14 Å. We therefore believe that nitryl group is significantly affect the inhibitory activity again the PDHc-E1. As expected, our experimental data support this proposes. As list in Table 1, when the nitryl group was taken into account, the IC_{50} value of compound **3b** is decreased 46.35 μM compared to compound **3c** (55.15 μM), which indicated that nitryl group on benzene ring significantly increases

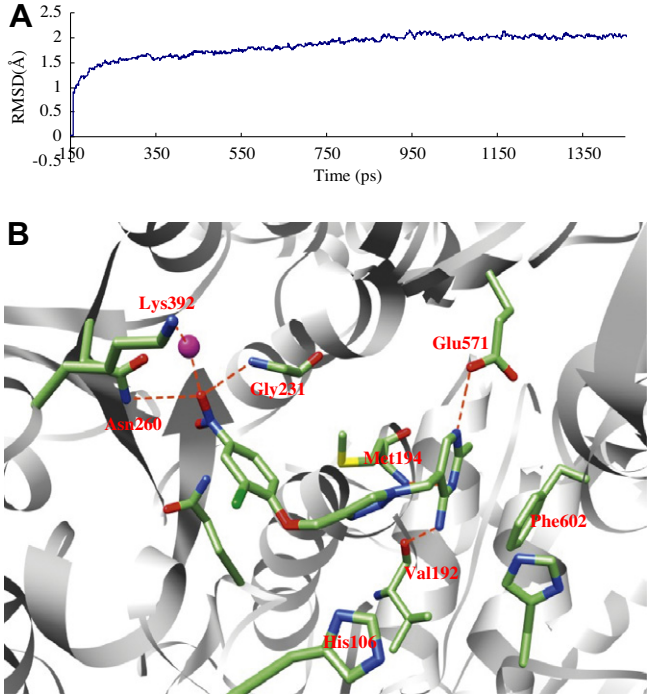

Figure 3. The results of MD simulation. (A) The MD simulation time versus root mean–square deviation (RMSD, in Å) of PDHc-E1 enzyme and compound **3a**. (B) Average conformation of PDHc-E1/compound **3a**, which was derived from the last 100 conformations in MD simulation. The coordinate bonds and hydrogen bonds are shown in dashed line (red).

the inhibitory activity of inhibitors. On the other hand, despite the docking result shows the chlorine atom on benzene can form one hydrogen bond with His106, the MD simulation disappeared this interaction, with a bond distance 5.52 Å. It suggest that the chlorine atom likely not important for the stabilizing of compound **3a**, thus we proposed that the chlorine atom is not a key factor to affect inhibitory activity of inhibitors. Our experimental results (Table 1) show that, when the chlorine atom was taken into account, the IC_{50} value of the compound **3a** decrease only about 2 μM compared to those of compound **3b** (8.88 μM).

In addition, the MD simulation also result in two hydrogen-bonds disappeared, the hydrogen-bond distance from compound **3a** to residues His640 and Lys392 increased more than 3 Å as compared with the docking results, especially, for the hydrogen-bond between nitryl group of benzene and residue Lys392, with a distance of 8.53 Å. This MD result also clearly suggests that both Lys392 and His640 are likely not important for the stabilization of these four inhibitors in the present study. By jointly using molecular docking and MD simulation, the relationship between the inhibitory activity and several functional groups can be reasonable explained, which lending credit to the reliability of active conformations obtained by SURFLEX module.

2.4. Binding energy and pair interaction analysis

To validate numerically the important interactions between ligand and specific amino acid residues obtained from molecular docking with SURFLEX and molecular dynamic simulation (MD), the pair interaction energies of compound **3a** with the binding sites of 1L8A were also investigated by using ab initio fragment molecular orbital (FMO) methods. The calculated pair interaction energies of compound **3a** with individual residue fragments in the selected active sites docked by SURFLEX module and simulated by MD method are illustrated in Figure 4(A and B).

As can be seen from Figure 4A and B, of all amino acid residues located in the active site of PDHc-E1, Mg^{2+} is responsible for the largest electrostatic contributions, it mainly due to the formation of strong coordinate-bond with electrostatic interaction type between the nitryl group on compound **3a** and Mg^{2+} with high positive charge. In addition, both the docking-based FMO and MD-based FMO calculations show that the charged residues Asp521, Glu522, Glu571, His640, His106, His142 and Asp230 exhibit the second largest electrostatic contributions to the stabilization of compound **3a**, because the stronger electrostatic interaction between compound **3a** and these residues with positive/negative charge centers can be found. We also noticed that the residues Cys259, Asn260, Arg263 and Leu264 exhibit large pair interaction energy, which mainly result from the steric clashes effect. It is conclude that most of the trends of pair interaction energies from both docking-based FMO and MD-based FMO are similar, such a similarity lends credit to the reliability of the model for SURFLEX docking and molecular dynamics simulations in the present work.

3. Conclusion

In the present study, with the effective docking process, four novel compounds with high inhibitory activity against PDHc-E1 from *E. coli* were designed by using structure-based docking. By jointly using the molecular dynamics simulation, and fragment molecular orbital (FMO) methods, the interaction mechanism between the active site of PDHc-E1 and its inhibitor was further investigated. The consistence between docking results and MD simulation results reveal that, the residues Glu571, Met194, Val192 and Phe602 are well conserved and might function in stabilization of aminopyrimidine on compound **3a**. Furthermore,

Table 2
The direct interactions between compound **3a** and residues in the active site of PDHc-E1 from *E. coli* for the docking conformation and docking-based MD conformation, respectively

Compound **3a**	Interaction	Distance (Å)			
		Residues	Docking	Docking-based MD	Residual error
Pyrimidine	H-bond	Glu571	2.00	1.87	−0.13
Pyrimidine	H-bond	Met194	2.25	2.71	0.46
Aminopyrimidine	H-bond	Val192	1.73	2.14	0.41
Pyrimidine	π–π stacking	Phe602	3.46	3.41	−0.05
Triazole	H-bond	His640	2.76	5.68	2.92
Chlorine group	H-bond	His106	2.91	5.52	2.61
Nityl group	Coordinate	Mg^{2+}	2.10	2.05	−0.05
Nityl group	H-bond	Gly231	2.29	3.41	1.12
Nityl group	H-bond	Lys392	2.30	8.53	6.23
Nityl group	H-bond	Asn260	2.24	2.80	0.56
Nityl group	H-bond	Gln140	6.37	2.14	−4.23

Table 1
The IC_{50} values of four compounds in the present study against PDHc-E1 from *E. coli*

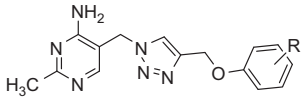

Compounds	R	IC_{50} (μM)
3a	2-Cl-4-NO_2	6.88
3b	4-NO_2	8.80
3e	4-COOH	15.10
3c	H	55.15

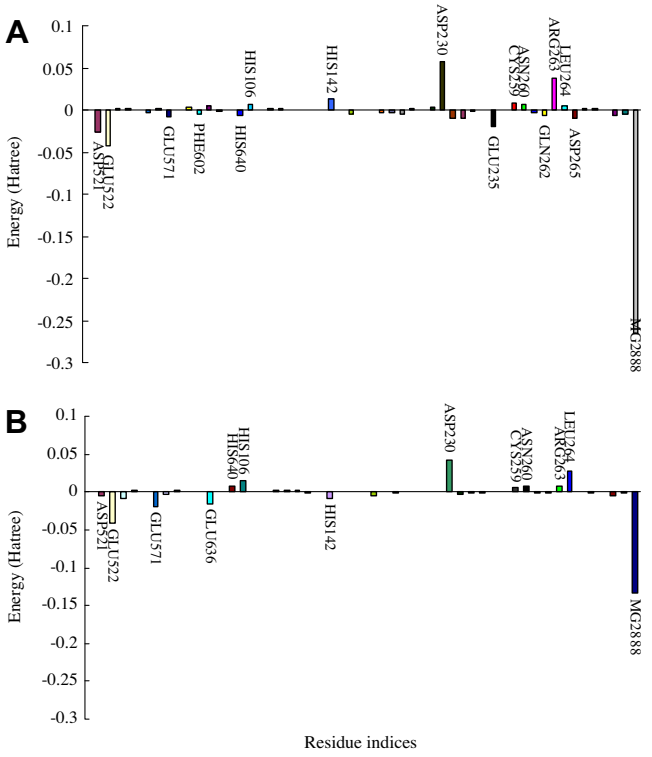

Figure 4. Comparison of pair interaction energies for compound **3a** calculated at FMO-RHF/6-31G* level, based on the docking-based conformation (A) and MD-based conformation (B), respectively.

the nitryl group on compound **3a** not only can form the hydrogen-bond with residue Asn260 but also can form coordinate-bond with Mg^{2+}, which is much important for stabilizing the compound **3a**. The representative four novel potential hit compounds with high inhibitory activities to PDHc-E1 components from *E. coli* were validated by the determination of IC_{50} values, which lends partial credit to the quality of molecular modeling strategy presented in this study. Our experimental results suggest that the nitryl group on compound **3a** is significantly affect the inhibitory activity again the PDHc-E1. The positive results indicated that all modeling strategies in the current study most like to be an encouraging way in find lead compounds with brand-new molecular backbone for the specifically individual pesticide as PDHc-E1 inhibitors in the future.

4. Experimental

4.1. Structure-based docking

For docking purposes, the crystallographic coordinates of the PDHc-E1 with bound ThDP from *E. coli* (PDB code: 1L8A) were obtained from Brookhaven Data Bank. Hydrogen atoms were added to the structure allowing for appropriate ionization at physiological pH. The protonated state of several important residues, such as His106, His142, Tyr599, Glu571 and His640, were adjusted by using SYBYL7.3 (Tripos, St. Louis, USA) in favor of forming reasonable hydrogen bond with the ligand. Molecular docking analysis was carried out by the SURFLEX module of SYBYL package to explore the interaction model for the active site of PDHc-E1 with its ligand, especially with cofactor ThDP. All atoms located within the range of 6.5 Å from any atom of the cofactor ThDP were selected into the active site, and the corresponding amino acid residue was, therefore, involved into the active site if only one of its atoms was selected. Other default parameters were adopted in the SURFLEX-docking calculations. All calculations were performed on a CCNUGrid-based computational environment (CCNUGrid website http://www.202.114.32.71:8090/ccnu/chem/platform.xml)

4.2. Molecular dynamics (MD) simulation

To confirm binding modes of hit compounds, the MD simulations were also performed by using SANDER module of AMBER 8.0 program package,[20] based upon the docking conformation of compound **3a**, to reduce steric clashes and obtain converged complexes structure of PDHc-E1 from *E. coli* and inhibitor. The leaprc.ff03 force field parameters were loaded into the PDHc-E1 enzyme system, the partial atomic charges of ligands were calculated by using the restricted electron-static potential (RESP)[21] fitting protocol implemented in the ANTECHAMBER module of AMBER 8.0 package. The whole system were first neutralized by adding Na^+ cation and then solvated into an octahedral box of TIP3P water molecules,[22] which extended about 10 Å

from any give atom of enzyme system of interest. The particle mesh Ewald method,[23,24] for the long-range electrostatics, a 10 Å cutoff for nonbonding van der Waals interactions, and periodic boundary conditions were set up for the following MD simulations. All bonds involving hydrogen were constrained using the SHAKE algorithm.[25] In addition, the following equilibration protocol was employed before starting the production-run phase. First, all water molecules of the TIP3P box were minimized 2500 steps by conjugate gradient, while holding the protein system frozen. Then, the protein systems were minimized by same strategy, while holding the water molecules of the TIP3P box frozen. Finally, the whole system (protein plus waters) were slowly heated from 10 to 298 K over 100 ps before MD simulation. Trajectories were recorded every 1 ps during the entire MD simulation process. An averaged structure of PDHc-E1 complexes include the inhibitor were derived from the trajectories of the last converged 100 ps, and subjected to a subsequent minimization using Tripos force field[26] of SYBYL7.3 with a rms gradient of 0.15 kcal/(mol Å) to adjust some unreasonable atoms.

4.3. Binding energy and pair interaction analysis

Based on the complexes structure of PDHc-E1 and inhibitor obtained by SURFLEX-docking and MD simulation, respectively, the pair interactions between specific amino acids of active site and inhibitors were calculated by using FMO method. It has been successfully applied for the quantum mechanical calculations of pair interaction energies of receptor with ligand.[27,28] For FMO methods, the whole molecular system is divided into small fragment, and ab initio MO calculations are performed on fragments and fragment pairs, which are referred to as 'monomers' and 'dimmers', respectively.[29–31]

In the present study, we adopted the residues located within a radius of 6.5 Å from the center of ligand in complex. The ends of the polypeptide fragments, $-NH_2$ was capped with hydrogen atoms, while the –CO was set to –COOH. To make the fragmentation of the receptor protein, the peptide chain was divided at the Cα atom into blocks of each residue in a manner. The ligand was treated as a single fragment.

All FMO calculation in the present study were performed by using ABINITMP package[30] at the HF/6-31G* level, other parameters adopted their default values.

4.4. Evaluation of inhibitory activity of PDHc-E1

The expressing plasmid pMal-C_{2X}-PDHc-E1 was transformed into *E. coli* stain TB1 and inoculated in Luria-Bertani (LB) broth containing 2% glucose and 30 mg/ml ampicillin at 37 °C until reaching a cell density to A600 of 0.6–0.8. Then cells were induced with a final concentration of 0.5 mM IPTG for 7 h at 25 °C before harvesting. Purification of the fusion protein was carried out using a MBP affinity column attached to an AKTA purifier 10 (UPC-F920, GE Healthcare Life Sciences). The concentrations of purified proteins were determined by the method of Bradford[32] using bovine serum albumin (Tiangen) as standard. The final purify (>95%) of the sample was verified by SDS–PAGE and then the purified protein was stored in 50% (v/v) glycerol at −20 °C.

The inhibitory activities of synthesized compounds were measured by the enzymatic assay. PDHc-E1 activity was assayed by a modified methods of N. Nemeria,[33] and measured by monitoring the reduction of 2,6-dichlorophenolindophenol (2,6-DCIP) at 600 nm using a microplate reader (BioTek Synergy2, USA). The total volume of 100 μL reaction mixture contained 50 mM K_3PO_4, pH7.2, 2.0 mM sodium pyruvate as substrate, 0.8 mM 2, 6-DCIP, 7.1 μM enzyme and different concentration of inhibitors. The reaction mixtures were incubated for 3 min at 37 °C, then added different concentration of ThDP (ranging from 0 to 200 μM) to initial reaction. The 50% inhibition concentration (IC_{50}) of synthesized compounds was estimated by non-linear least-squares fitting of the data using the logarithmic regression curves. One unit of activity is defined as the amount of 2, 6-DCIP reduced (μmol/min/mg of PDHc-E1). The compounds structures and corresponding IC_{50} values of four compounds were list in Table 1, respectively. Experimentally, all of our designed four compounds exhibit rather high inhibition activity, with IC_{50} value of 6.88, 8.80, 11.35 and 55.15 μM. These results revealed that these four hit compounds have more potent inhibition to the PDHc-E1 enzyme.

4.5. Synthesize

Melting points (mp) were measured on an electrothermal melting point apparatus and were uncorrected. ^{1}H NMR spectra were recorded at 400 MHz or 600 MHz, in $CDCl_3$ or DMSO-d_6 solution on a Varian Mercury-Plus 400 or 600 spectrometer and chemical shifts were recorded in parts per million (ppm) with TMS as the internal reference. Mass spectra (MS) were obtained on a QTRAP LC/MS/MS system (API2000; Applied Biosystems, Foster City, CA, USA). Elemental analysis (EA) was measured on a Vario ELIII CHNSO elemental analyzer. Unless otherwise noted, reagents were purchased from commercial suppliers and used without further purification. Intermediate **2** was synthesized according to the existing methods.[18]

4.5.1. General procedure for preparation of compounds 3a–3d

A solution of 3-bromopropyne (0.71 g, 6 mmol), corresponding substituted phenol (5 mmol) and K_2CO_3 (1.38 g, 10 mmol) in acetone (20 mL) was heated under reflux until the reaction was complete based on TLC monitoring. Then the solvent was removed under reduced pressure. The residue was dissolved in water and aqueous layer was extracted twice with dichloromethane. The combined organic phases were dried with $MgSO_4$ and evaporated at reduced pressure to obtain crude product, which was used directly for the next step reaction without further purification.

To a stirred solution of 5-azidomethyl-2-methylpyrimidine-4-ylamine **3** (1 mmol, 1.0 equiv) and substituted (prop-2-yn-1-yloxy)benzene **1a–1d** (1.1 mmol, 1.1 equiv) in *tert*-butanol/water (9 mL, 2:1) were added sodium ascorbate (99 mg, 0.5 mmol) and $CuSO_4{\cdot}5H_2O$ (12.5 mg, 0.05 mmol). The reaction mixture was stirred at room temperature for 12 h. It was poured into cold water (50 mL), and the precipitate was collected by filtration and dried in the atmospheric pressure. Recrystallization with appropriate solvent afforded the desired solid compounds **3a–3d**.

4.5.1.1. 5-((4-((2-Chloro-4-nitrophenoxy)methyl)-1H-1,2,3-triazol-1-yl)methyl)-2-methylpyrimidin-4-amine (3a). Yellow solid; yield 81%; mp 194–196 °C. ^{1}H NMR (600 MHz, DMSO-d_6) δ (ppm): 2.32 (s, 3H, CH_3), 5.43 (s, 2H, OCH_2), 5.47 (s, 2H, CH_2), 6.96 (s, 2H, NH_2), 7.61-7.62 (d, 1H, J = 7.2 Hz, Ar-H), 8.03 (s, 1H, triazole-CH), 8.27 (s, 1H, pyrimidine CH), 8.29–8.30 (d, 1H, J = 6.6 Hz, Ar-H), 8.32–8.33 (s, 1H, Ar-H). ESI-MS m/z: 376 $(M+1)^+$. Anal. calcd for $C_{15}H_{14}ClN_7O_3$: C, 47.94; H, 3.76; N, 26.09. Found: C, 47.39; H, 3.74; N, 25.82.

4.5.1.2. 2-Methyl-5-((4-((4-nitrophenoxy)methyl)-1H-1,2,3-triazol-1-yl)methyl)pyrimidin-4-amine (3b). Yellow solid; yield 79%; mp 202–204 °C. ^{1}H NMR (600 MHz, DMSO-d_6) δ (ppm): 2.31 (s, 3H, CH_3), 5.31 (s, 2H, OCH_2), 5.46 (s, 2H, CH_2), 6.95 (s, 2H, NH_2), 7.25–7.26 (d, 2H, J = 9.0 Hz, Ar-H), 8.02 (s, 1H, triazole CH), 8.21–8.22 (d, 2H, J = 9.6 Hz, Ar-H), 8.27 (s, 1H, pyrimidine CH). ESI-MS m/z: 342 $(M+1)^+$. Anal. calcd for $C_{15}H_{15}N_7O_3$: C, 52.78; H, 4.43; N, 28.73. Found: C, 52.53; H, 4.33; N, 28.22.

4.5.1.3. 2-Methyl-5-((4-(phenoxymethyl)-1H-1,2,3-triazol-1-yl) methyl)pyrimidin-4-amine (3c). White solid; yield 90%; mp 132–133 °C. ^{1}H NMR (600 MHz, $CDCl_3$) δ (ppm): 2.50 (s, 3H, CH_3), 5.18 (s, 2H, OCH_2), 5.35 (s, 2H, CH_2), 5.59 (s, 2H, NH_2), 6.95–6.99 (m, 3H, Ar-H), 7.27–7.30 (t, 2H, J = 7.8 Hz, Ar-H), 7.62 (s, 1H, triazole CH), 8.19 (s, 1H, pyrimidine CH). ESI-MS *m/z*: 297 $(M+1)^+$. Anal. calcd for $C_{15}H_{16}N_6O$: C, 60.80; H, 5.44; N, 28.36. Found: C, 60.62; H, 5.35; N, 28.60.

4.5.1.4. Ethyl 4-((1-((4-amino-2-methylpyrimidin-5-yl)methyl)-1H-1,2,3-triazol-4-yl)methoxy)benzoate (3d). White solid; yield 94%; mp 190–192 °C. ^{1}H NMR (400 MHz, DMSO-d_6) δ (ppm):1.28-1.31 (t, 3H, J = 10.2 Hz, 10.8 Hz, CH_3), 2.30 (s, 3H, CH_3), 4.24–4.29 (q, 2H, J = 10.8 Hz, CH_2), 5.22 (s, 2H, OCH_2), 5.45 (s, 2H, CH_2), 6.93 (s, 2H, NH_2), 7.12-7.14 (d, 2H, J = 12.6 Hz, Ar-H), 7.89–7.91 (d, 2H, J = 12.6 Hz, Ar-H), 8.01 (s, 1H, triazole-CH), 8.24 (s, 1H, pyrimidine CH). ESI-MS *m/z*: 369 $(M+1)^+$. Anal. calcd for $C_{18}H_{20}N_6O_3$: C, 58.69; H, 5.47; N, 22.81. Found: C, 58.88; H, 5.59; N, 22.62.

4.5.2. Procedure for preparation of compound 3e

The stirred reaction mixture of **3d** (0.37 g, 1 mmol) and LiOH monohydrate (126 mg, 3 mmol) dissolved in THF/MeOH/H_2O (2:1:1, 12 mL) was stirred at room temperature until the reaction was complete based on TLC monitoring. Then the solvent was removed under reduced pressure. The residue was dissolved in water and quench the mixture with dilute HCl solution to pH = 3. The precipitate was collected by filtration, washed with little THF and dried in the atmospheric pressure.

4.5.2.1. 4-((1-((4-Amino-2-methylpyrimidin-5-yl)methyl)-1H-1,2,3-triazol-4-yl)methoxy)benzoic acid (3e). White solid; yield 76%; mp >260 °C. ^{1}H NMR (400 MHz, DMSO-d_6) δ (ppm): 2.34 (s, 3H, CH_3), 5.22 (s, 2H, OCH_2), 5.47 (s, 2H, CH_2), 7.11–7.13 (d, 2H, J = 13.2 Hz, Ar-H), 7.20 (s, 2H, NH_2), 7.88–7.90 (d, 2H, J = 12.6 Hz, Ar-H), 8.06 (s, 1H, triazole-CH), 8.26 (s, 1H, pyrimidine CH). ESI-MS *m/z*: 341 $(M+1)^+$. Anal. calcd for $C_{16}H_{16}N_6O_3$: C, 56.47; H, 4.74; N, 24.69. Found: C, 56.35; H, 4.74; N, 24.45.

Acknowledgments

This work was supported by the National Basic Research Program of China (973 Program, No. 2010CB126100), the Natural Science Foundation of China (Nos. 20873049, 20872044, 21072073, 21172089, 20372023 and 21172090), Natural Science Foundation of Hubei Province (No. 2010CDB01202), the Program for Academic Leader in Wuhan Municipality (No. 201150530150), the self-determined research funds of CCNU from the colleges' basic research and operation of MOE (Nos. CCNU09A01010, CCNU10C01002, and CCNU10A02006), and the research was also supported in part by the PCSIRT (No. IRT0953).

References and notes

1. Wei, W.; Li, H.; Nemeria, N.; Jordan, F. *Protein Expr. Purif.* **2003**, *28*, 140.
2. Baillie, A. C.; Wright, K.; Wright, B. J.; Earnshaw, C. G. *Pestic. Biochem. Physiol.* **1988**, *30*, 103.
3. Bisswanger, H. *Eur. J. Biochem.* **1974**, *48*, 377.
4. Lowe, P. N.; Perham, R. N. *Biochemistry* **1984**, *23*, 91.
5. Flournoy, D. S.; Frey, P. A. *Biochemistry* **1989**, *28*, 9594.
6. Bisswanger, H. *Biochem. Biophys. Res. Commun.* **1980**, *95*, 513.
7. Kluger, R.; Pike, D. C. *J. Am. Chem. Soc.* **1977**, *99*, 4504.
8. Schoenbrunn-Hanebeck, E.; Laber, B.; Amrhein, N. *Biochemistry* **1990**, *29*, 4880.
9. Adamson, S. R.; Stevenson, K. J. *Biochemistry* **1981**, *20*, 3418.
10. Adamson, S. R.; Robinson, J. A.; Stevenson, K. J. *Biochemistry* **1984**, *23*, 1269.
11. Jackson, R. H.; Singer, T. P. *J. Biol. Chem.* **1983**, *258*, 1857.
12. Brown, A.; Nemeria, N.; Yi, J.; Zhang, D.; Jordan, W. B.; Machado, R. S.; Guest, J. R.; Jordan, F. *Biochemistry* **1997**, *36*, 8071.
13. Apfel, M. A.; Ikeda, B. H.; Speckhard, D. C.; Frey, P. A. *J. Biol. Chem.* **1984**, *259*, 2905.
14. Maldonado, M. E.; Oh, K.-J.; Frey, P. A. *J. Biol. Chem.* **1972**, *247*, 2711.
15. Lowe, P. N.; Leeper, F. J.; Perham, R. N. *Biochemistry* **1983**, *22*, 150.
16. Gutowski, J. A.; Lienhard, G. E. *J. Biol. Chem.* **1976**, *251*, 2863.
17. Arjunan, P.; Nemeria, N.; Brunskill, A.; Chandrasekhar, K.; Sax, M.; Yan, Y.; Jordan, F.; Guest, J. R.; Furey, W. *Biochemistry* **2002**, *41*, 5213.
18. Erixon, K. M.; Dabalos, C. L.; Leeper, F. J. *Org. Biomol. Chem.* **2008**, *6*, 3561.
19. Rostovtsev, V. V.; Green, L. G.; Fokin, V. V.; Sharpless, K. B. *Angew. Chem., Int. Ed.* **2002**, *41*, 2596.
20. Case, D. A.; Darden, T. A.; Cheatham, T. E.; Simmerling, C. L.; Wang, J.; Duke, R. E.; Luo, R.; Merz, K. M.; Wang, B.; Pearlman, D. A.; Crowley, M.; Brozell, S.; Tsui, V.; Gohlke, H.; Mongan, J.; Hornak, V.; Cui, G.; Beroza, P.; Schafmeister, C.; Caldwell, J. W.; Ross, W. S.; Kollman, P. A. **2004** AMBER 8, University of California, San Francisco.
21. Wang, J. M.; Wang, W.; Kollman, P. A. *Abstr. Pap. Am. Chem. Soc.* **2001**, *222*, U403.
22. Jorgensen, W. L.; Chandrasekhar, J.; Madura, J. D.; Impey, R. W.; Klein, M. L. *J. Chem. Phys.* **1983**, *79*, 926.
23. Darden, T.; York, D.; Pedersen, L. *J. Chem. Phys.* **1993**, *98*, 10089.
24. Essmann, U.; Perera, L.; Berkowitz, M. L.; Darden, T.; Lee, H.; Pedersen, L. G. *J. Chem. Phys.* **1995**, *103*, 8577.
25. Ryckaert, J.-P.; Ciccotti, G.; Berendsen, H. J. C. *J. Comput. Phys.* **1977**, *23*, 327.
26. Clark, M.; Cramer, R. D.; Van Opdenbosch, N. *J. Comput. Chem.* **1989**, *10*, 982.
27. Nemoto, T.; Fedorov, D. G.; Uebayasi, M.; Kanazawa, K.; Kitaura, K.; Komeiji, Y. *Comput. Biol. Chem.* **2005**, *29*, 434.
28. Yamagishi, K.; Yamamoto, K.; Yamada, S.; Tokiwa, H. *Chem. Phys. Lett.* **2006**, *420*, 465.
29. Kitaura, K. *Chem. Phys. Lett.* **1999**, *313*, 701.
30. Komeiji, Y.; Inadomi, Y.; Nakano, T. *Comput. Biol. Chem.* **2004**, *28*, 155.
31. Nakano, T.; Kaminuma, T.; Sato, T.; Fukuzawa, K.; Akiyama, Y.; Uebayasi, M.; Kitaura, K. *Chem. Phys. Lett.* **2002**, *351*, 475.
32. Bradford, M. M. *Anal. Biochem.* **1976**, *72*, 248.
33. Nemeria, N.; Yan, Y.; Zhang, Z.; Brown, A. M.; Arjunan, P.; Furey, W.; Guest, J. R.; Jordan, F. *J. Biol. Chem.* **2001**, *276*, 45969.